myjournal manuscript No.
(will be inserted by the editor)

First Order Phase Change Detection Using Planar Waveguide Bragg Grating Refractometer

I.J.G.Sparrow[1], G.D.Emmerson[2], C.B.E.Gawith[1], P.G.R.Smith[1], M.Kaczmarek[3], A.Dyadyusha[3]

[1] Optoelectronics Research Centre, University of Southampton, Southampton, UK
[2] Stratophase Ltd, Romsey, Hampshire, SO51 9AQ, UK
[3] School of Physics and Astronomy, University of Southampton, Southampton, UK

Received: date / Revised version: date

Abstract Solid-to-liquid and gas-to-liquid phase changes in water and ordered-to-isotropic phase changes in a nematic liquid crystal are detected with an optical sensor. A planar Bragg grating defined purely by refractive index modulation is covered with a water or liquid crystal overcladding and the temperature is controlled to trigger phase changes. Measurement of the Bragg wavelength allows changes of effective refractive index to be detected and discontinuities in behaviour caused by phase transitions can be clearly identified.

1 Introduction

Optical sensors for fundamental measurements of physical and chemical properties have received considerable interest in recent years [1] [2] and the goal of a lab-on-a-chip is often quoted. Temperature, pH, chemical, and material state changes are all measurements of interest for both research and industrial purposes. Various optical techniques have been developed for a range of technologies and applications, including the detection of scatter from particles [3], surface plasmon resonance [4], mach-zehnder interferometers [5], grating couplers [1] [6], relief gratings [7], long period gratings [8] and fibre bragg grating sensors [9].

Here, we present a planar waveguide sensor capable of directly detecting small changes in refractive index. The use of refractive index changes to vary an optical waveguide response is not new and comparable work using relief gratings over optical waveguides [7] [9] and Fibre Bragg gratings [9] has been presented. However, the full potential of such devices has not been exploited and planar geometries have received remarkably little attention. One advantage of the planar waveguide approach over fibre is the possibility for integration. Multiple sensors can be realised on a single chip using standard clean room procedures and the end product can be more robust than the etched fibre equivalents which can often be fragile. Additionally, the UV writing approach used here [10] simplifies fabrication and allows Bragg gratings to be defined purely by refractive index modulation, resulting in a smooth, homogeneous and easily cleaned upper surface. A feature of the technique used here is that the definition of waveguides and gratings is carried out entirely under software control. Consequently, modifications to the grating or waveguide structures can be made simply by providing the correct instruction set to the UV writing system. In contrast, alternative routes to creating planar Bragg structures require photolithographic techniques to create masks for either relief etching or UV exposure. Etched gratings require are susceptible to contamination between grating planes, have inherent structure related stress and are at risk of damage due to expansion and contraction of water within the etched structure. This is the first time that such an optical device has been used to detect phase transitions in a material.

Phase changes can be grouped into first order or second order transitions. First order transitions such as the melting and evaporation of water or the transition between isotropic and nematic liquid crystal states [11], are characterised by a discrete change in thermodynamic order and have an associated latent heat. The change in order of the substances can be expected to have an associated change of refractive index, the property that is measured here.

Key to the sensitivity of this technique are Bragg gratings defined in an optical waveguide. The wavelength of a Bragg grating reflection (or transmission) peak is given by

$$\lambda_b = 2\Lambda n_{eff} \tag{1}$$

Where λ_b is the Bragg wavelength, n_{eff} provides the effective refractive index and Λ is the period of the refractive index modulation that defines the grating. The value of n_{eff} is determined by the magnitude of the index modulation and also, due to evanescent field interaction, by the refractive index of the waveguide core

and cladding. Thus, with the underclad and core layer unchanged, it is possible to control the reflection wavelength of a Bragg grating by variation of the refractive index of the overclad. As long as the evanescent field of the guided mode penetrates the material being studied, small changes in the refractive index of the material will affect the effective index of the grating.

The technique used here is localised removal and replacement of the overcladding with an analyte directly above a Bragg grating. Using a commercially available optical spectrum analyser to measure the central wavelength of the grating response, changes in the effective refractive index of less than 1×10^{-5} can be determined. Variations of this magnitude are found to allow easy detection of phase transitions. Controlling the temperature of the device, whilst monitoring the associated changes in index, provides information on the material behaviour over the temperatures used.

2 Fabrication

Two samples were used in this work, one for monitoring atmospheric moisture condensation, the other for liquid crystal phase change detection. Both were fabricated using the same methods and equipment. The planar waveguide samples are three layer silica on silicon fabricated by flame hydrolysis deposition and subsequently exposed to a 244nm CW laser to define the waveguiding structures. The direct UV writing approach is a flexible route to device fabrication and has the added advantage that Bragg gratings can be written into the sample at the same time and under the same conditions as the waveguide itself [10]. Here, the gratings were defined with a period of 537nm and when covered with analyte displayed a Bragg resonance at approximately 1560nm. To provide UV photosensitivity in the core layer, it is co-doped with germanium. On exposure to a focused UV laser spot the material exhibits a localised refractive increase. Translation of the sample beneath the focused spot allows an optical waveguide to be written. The use of two beams focused onto the same spot creates an interference pattern which can be transferred into the induced refractive index profile of the germanium doped silica layer. Modulation of the laser beam, with the correct timing relative to the translation speed and the inherent period of the interference pattern, provides the Bragg grating that is key to these devices.

To make the samples suitable for detection of material properties, the upper layer of the sample was etched, using hydrofluoric acid and a simple etch mask, subsequent to UV exposure. By careful timing of the etch stage, approximately 20 microns of the upper layer is removed in the vicinity of the Bragg grating section of the waveguide as shown in Fig. 1. Both samples used were pigtailed with single mode telecoms fibre in order to avoid variation in fibre to waveguide coupling over

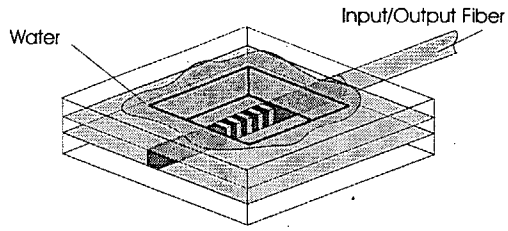

Fig. 1 Schematic representation of fibre couple three layer sample with water (or liquid crystal) over Bragg grating.

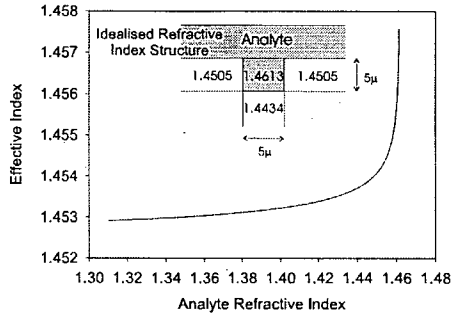

Fig. 2 Modelled variation of effective index with analyte refractive index for idealised step index waveguiding structure.

the temperature ranges used. As with all asymmetric waveguide sensing structures of this nature the devices have significantly higher birefringence than symmetric fibre designs. To overcome this, a polarisation controller was used to select and hold the polarisation to provide optimum reflection strength at the Bragg wavelength.

3 Advantages and Limitations

Owing to the use of silica waveguiding technology there are very few restrictions on the analytes that can be studied using this method. The silica surface is resistant to many acids, is easily cleaned and stable to high temperatures. The main limitation on the use of such a sensor is with high refractive index substances which have the potential to cause the guided optical mode to leak out of the waveguide core resulting in a very high loss device leading to poor signal levels.

As already mentioned in section 1, planar geometries for refractometers are advantageous as they allow integration of multiple functions. In turn this also allows such devices to operate over a wide range of environmental conditions. For example, to compensate for variable environmental temperatures non-exposed reference gratings operating at a different Bragg wavelengths can be easily included into the sensor design [12]. This allows temperature, stress and long term ageing effects of the substrate to be detected as an independent Bragg wavelength shift and then compensated for. The output of the exposed Bragg grating device response is such that an increase in refractive index always increases the effective index and therefore the Bragg wavelength. This allows

for simple interpretation of the results and avoids the need for multiple output devices as used, for example in [5] to overcome the cyclic response to variations in refractive index. As both device styles rely on modification of effective index by an analyte overlayer the theoretical limit of resolution is comparable. However, waveguide parameters and methods of processing results must be taken into account when making direct comparisons of devices.

Fig. 2 shows how the effective modal index of an idealised step-index waveguide responds to changes in analyte index. The waveguide indices and dimensions used are typical of a UV written structure and have been modelled using the Marcatili method [13]. Known effective indices presented in section 5 have been used to provide reference points upon which to base the modelled data of fig. 2. Experimental values of the effective index with analytes of n=1 (air) and n=1.31 (water) were used for this. The graph of Fig. 2 shows the variation of device sensitivity with analyte refractive index. The sensitivity of effective index to a modulation of analyte refractive index is given by the gradient of the curve. With an analyte index of 1.4606 the ratio of analyte modulation to effective index change is approximately unity. As fig. 2 shows this drops rapidly with decreasing analyte index. At the refractive index of water (approximately 1.31 at 1560nm) the modelled sensitivity is reduced by a factor of approximately 500. Even with this reduced sensitivity, our model predicts that the typical wavelength resolution of an optical spectrum analyser (10pm) allows the detection of refractive index changes in water of 5×10^{-3} or lower despite its relatively low refractive index.

Ultimately, the smallest measurable increment in refractive index is determined by the measurement technique in use. The non-specialist hardware used for this work has proven to allow clear identification of the behaviour of the analytes used.

4 Liquid Crystal Phase Detection

It is well known that the level of order displayed in liquid crystals can be altered with temperature and often with applied electric field [11]. One of the characteristics of nematic liquid crystals is that the long chain molecules statistically tend to orient themselves along a preferred axis, known as the director, causing birefringence in the liquid. Without the influence of external factors, such a liquid crystal will appear cloudy due to localised director variations causing scattering. Increasing the temperature of the liquid will result in increased molecular vibration and at a given temperature, known as the clearing point, the local order is lost leaving the liquid with no preferential director axis. The clearing point marks the change from a liquid crystal with some level of local order, to an isotropic liquid.

The liquid crystal used in this work was Merck 18523, carefully chosen for its refractive index compatibility

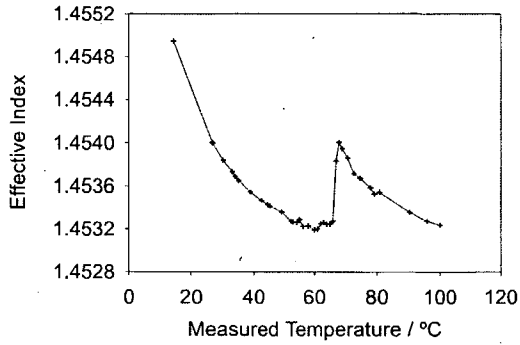

Fig. 3 Variation of effective index with temperature of Bragg grating with liquid crystal overclad.

with the silica used to fabricate the sensors. At 589nm the liquid crystal extraordinary and ordinary refractive indices are 1.5089 and 1.4599 respectively, and have been estimated [14] at 1.489 and 1.444 at 1550nm.

The liquid crystal was simply applied to the upper surface of the device over the waveguide core containing the refractive index grating and was not constrained either by side walls or an overlayer. No treatments were applied to influence the liquid crystal director orientation. The whole arrangement was mounted onto a heater and the temperature monitored using a thermocouple positioned below the sensor. Reflection spectra were recorded from the sample as it was heated between room temperature and 100°C. Measurements were also taken as the sample cooled to check for hysteresis in the response. The results of these measurements are displayed in Fig. 3. The data shows a general decrease in effective index of the Bragg grating with temperature, detected as a decrease in the wavelength of the Bragg reflection peak. A significant feature of the data is the very sharp discontinuity at 66°C. This clearly shows the liquid crystal to liquid phase transition between ordered and isotropic states and is characteristic of a first order transition. Visual determination of the clearing point by heating a vial of the liquid crystal determined that the transition occurred just above 60°C, the slight discrepancy explained by the position of the thermocouple relative to the grating surface when recording spectra. No hysteresis was observed when cooling. The temperature response of the grating without any overlayer was a linear variation with a temperature coefficient of 11 pm C^{-1}.

5 Water Phase Detection

To allow condensation of atmospheric water on the silica surface the device was mounted, adjacent to a thermocouple, on a peltier device to allow cooling. As with the liquid crystal, a temperature offset can be expected between the surface of the grating and the thermistor used, the magnitude of which is easily determined by comparison of the results with the known melting point

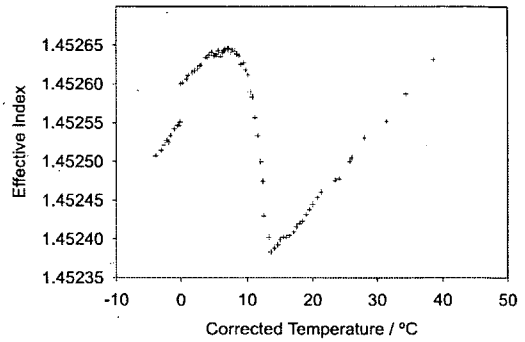

Fig. 4 Variation of effective index with corrected temperature due to condensation of atmospheric water.

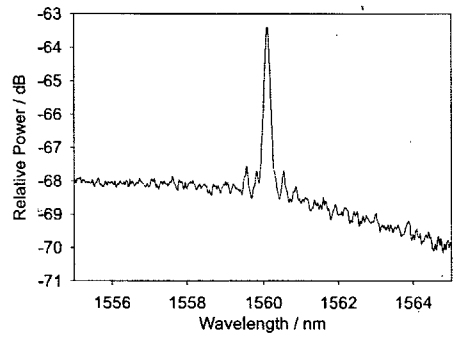

Fig. 5 Reflection spectrum of sensor covered in frozen water.

of water. The results of allowing water to condense onto the exposed grating are shown in Fig. 4 and a measured reflection spectrum in Fig. 5. Condensation will form continuously below a given temperature under constant ambient conditions. To allow for this, successive spectra were taken approximately ninety seconds apart with a corresponding temperature change of approximately 0.3°C. The temperature scale shown in the figure is corrected by 4.0 degrees to compensate for the temperature offset between grating and thermistor. The data shows the expected linear grating response with temperature above 14°C. Below this temperature condensation could be seen beginning to form on the surface of the sample and a corresponding increase in effective index is seen. As the temperature decreases further, the effective index begins to level off and then decrease as the water layer over the grating becomes a continuous layer and the index temperature dependence of water becomes dominant over the increasing volume of water. As predicted, when freezing, the condensed water causes a discontinuity in the effective index. The drop in effective index is due to the density change between water and ice. Ice is known to be less dense than water and so the lower index is expected. The condensation section of Fig. 4, between 14 and 8 °C, highlights the high sensitivity of the technique as the formation of water droplets can be seen as a gradual process. These results demonstrate that the technique not only indicates the presence of water but also shows the build up of the water layer and allows the intermediate state between no water and a pool of water to be monitored. Such sensitivity could have significant uses in monitoring the progress of chemical reactions or moisture levels in critical storage applications.

6 Conclusions

The presented results show that we have developed a sensitive means of detecting and monitoring phase changes with a planar waveguiding device. The examples shown here demonstrate that liquid-solid, gas-liquid and liquid-liquid transitions can be clearly identified using the Bragg wavelength of reflection spectra. Such sensors require only a single mode optical fibre input and so can be positioned remotely in a variety of applications. The non-discrete transition from gaseous to condensed water highlights the ability to measure continuous processes with high sensitivity. Additional calibration work should allow the thickness or mass of water, or other chemical, over the sensor to be determined. Further areas for study include the detection of continuous phase transitions such as the change from smectic to nematic liquid crystal phase which is typically of second order.

References

1. W.Lukosz, Sensors Actuators B **29,** (1995) 37-50.
2. R.A.Yotter and L.A.Lee and D.M.Wilson, IEEE Sensors Journal, yotter **4,** (2004) 395-411.
3. S.G.Demos and R.R.Alfano, Elec. Lett., **32,** (1996), 2254-2255.
4. J.Homola, S.S.Yee and G.Gauglitz, Sensors Actuators B., **54,** (1999), 3-15.
5. B.J.Luff, J.S.Wilkinson, J.Piehler, U.Hollenbach, J.Ingenhoff and N.Fabricius", J. Lightwave Technol., **16,** (1998), 583-592.
6. K.Tiefenthaler and W.Lukosz, J. Opt. Soc. Am. B, **6,** (1989) 209-220.
7. G.J.Veldhuist, J.H.Berends, R.G.Heideman and P.V.Lambeck, Pure App Opt **7,** (1998), L23-L26.
8. V.Bhatia and A.M.Vengsarkar, Opt. Lett. **21,** 1996, 692-694.
9. A.Asseh, S.Sandgren, H.Åhlfeldt, B.Sahlgren, R.Stubbe and G.Edwall, Fiber and Integrated Optics **17,** (1998) 51-62.
10. G.D.Emmerson, S.P.Watts, C.B.E.Gawith, V.Albanis, M.Ibsen, R.B.Williams and P.G.R.Smith, Elec. Lett. **38,** (2002) 1531-1532.
11. D.Demus, J.Goodby, G.W.Gray, H.-W.Spiess and V.Vill, *Handbook of Liquid Crystals: Vol.1: Fundamentals* (Wiley-VCH, 1998)
12. K.Schroeder, W.Ecke, R.Mueller, R.Willsch and A.Andreev, Meas. Sci. Technol. **12,** (2002) 757-764.
13. E.A.J.Marcatili, Bell Syst. Tech. J., **48,** (1969) 2071-2102.
14. R.-P.Pan, S.-R.Liou and C.-K.Lin, Jpn. J. Appl. Phys. **34,** 1995, 6410-6415.